

WHY IS CERES LUMPY? SURFACE DEFORMATION INDUCED BY SOLID-STATE SUBSURFACE FLOW. M. T. Bland¹, H. G. Sizemore², D. L. Buczkowski³, M. M. Sori⁴, C. A. Raymond⁵, S. D. King⁶, C. T. Russell⁷. ¹USGS Astrogeology Science Center, Flagstaff AZ (mbland@usgs.gov). ²Planetary Science Institute, Tucson AZ. ³Johns Hopkins University Applied Physics Lab., Laurel MD. ⁴University of Arizona, Tucson AZ. ⁵JPL Caltech, Pasadena CA. ⁶Virginia Tech., Blacksburg VA. ⁷UCLA, Los Angeles CA.

Overview: Portions of Ceres' surface are marked by numerous large domes and irregular mounds (tholi), resulting in "lumpy" topography. The formation of these tholi is uncertain, but cryovolcanism and subsequent viscous relaxation has previously been suggested [1, 2]. Here we propose an alternate hypothesis: tholi form by solid-state flow of relatively low viscosity and low density material in a crust that is compositionally heterogeneous over large (e.g., km) scales. We show that flow driven by a combination of differential loading and buoyancy can partially account for these unique topographic features.

Tholi on Ceres: Portions of Ceres' surface contain numerous large (>10 km diameter) domes and irregular mounds [3, 4] (here we refer to them collectively as tholi). The tholi range from domical with circular planform, to highly irregular in shape, with typical effective maximum diameters of 20–100 km [3]. Tholi relief is generally 2–4 km. Tholi are not distributed uniformly across Ceres, but rather are concentrated between longitudes 270° and 15° (Fig. 1 and [4]). This region is much lower (relative to the best fit ellipsoid) than areas to the west (Hanami Planum) or east, and may be associated with an ancient impact basin [5]. Ahuna Mons, which may be the youngest example of such features on Ceres, occurs in this region [1, 2]. Several other notable examples occur within the interior of craters, such as Cosecha Tholus and an unnamed tholus in Begbalel crater.

Formation of Ceres' tholi: Previously, it was suggested that Ceres' tholi might form by cryovolcanic emplacement of steep-sided domes, as proposed for Ahuna Mons [1], followed by subsequent viscous relaxation of the topography [2]. Here we propose an alternative mechanism: solid-state flow of a low-viscosity component within Ceres' heterogeneous crust. As a direct analog, we use concepts from terrestrial salt tectonics (which have also been applied to Mars [e.g., 6 and several others]), in which lower-viscosity/density (LV-LD) salt layers deform overlying, higher-viscosity/density (HV-HD) strata into domes: features similar to those observed on Ceres. Salt tectonics is driven by a combination of buoyancy, differential loading, and regional tectonism [e.g., 7].

Ceres' heterogeneous crust. Previous work has shown that Ceres' crust (the ~40 km thick outer, lower-density layer [8]) is a mixture of rock, ice, salts, and

clathrate [9, 10]. Whereas those studies assumed a well-mixed composition, variations in viscous relaxation [9], surface composition [11], surface morphology [12], and gravity [8] across Ceres suggest possible large-scale (km to 10s of kms) compositional heterogeneity. Here we assume that Ceres' crust is heterogeneous at these large scales, and that these variations are reflected in differences in density and viscosity. Below we examine whether such heterogeneity might result in the deformation of Ceres' surface.

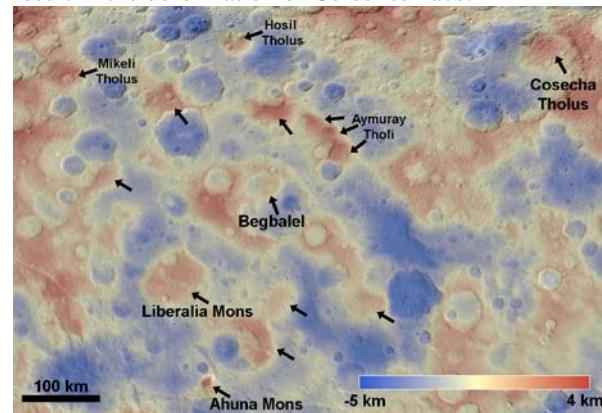


Figure 1: A portion of Ceres (285°-20° longitude) exhibiting numerous tholi and montes (black arrows indicate prominent features, some labeled). Color-coded topography overlain on a 140 m/pix image mosaic.

Buoyancy-driven diapirs. Although now recognized as a minor driver of salt tectonics [7], buoyancy forces might play a crucial role in solid-state deformation on Ceres. To test this hypothesis, we posit a spherical ice diapir (density $\rho_i = 920 \text{ kg m}^{-3}$) within Ceres' higher density crust ($\rho_c = 1287 \text{ kg m}^{-3}$ [8]). To first order, the upward velocity of the sphere depends on its radius R , the density contrast $\Delta\rho$, gravity ($g=0.27 \text{ m s}^{-2}$), and the viscosity of the crust, which is a function of temperature and thus depth ($\eta(z)$). We assume the viscosity structure of [10] and integrate to determine the time required for the diapir to reach the surface. We find that diapirs with $R < 100 \text{ km}$ (considered a maximum) cannot reach Ceres' surface over geologic time due to the high viscosity of the near-surface crust. This result is independent of the depth at which the diapir initiates. Large diapirs can, however, reach depths of 10–20 km before stalling out, suggesting that low density material may not remain at the

base of the crust, but can accumulate at shallower depths.

Deformation driven by differential loading. Most salt tectonics on Earth is driven by differential loading or regional tectonics [7]. Given the general lack of evidence for tectonic activity on Ceres, we examine the role of differential loading (flow driven by a hydraulic head) in creating Ceres' tholi. A pressure head is created by lateral variation in the thickness of the HV-HD crust overlying the LV-LD material, either due to changes in the LV-LD layer thickness (case 1, Fig. 2) or to surface topography (case 2, Fig. 3). We examine both cases using a simple viscoelastic finite element model (Tekton [13]) in axisymmetric geometry. We assume a subsurface LV-LD layer beneath (or within) an HV-HD crust.

In case 1, the difference in the LV-LD layer thickness is a simple step function, creating a vertical column of LV-LD material (designed after [14]). We find that the presence of this column can result in significant uplift of the surface. For the case shown in Fig. 2, the result is a tholus ~2 km high and 20 km across. The degree to which the surface deforms depends strongly on the initial geometry. Wider LV-LD columns, and thinner overlying HV-HD layers produce greater uplift, suggesting broad tholi are easier to produce by this mechanism than small, narrow tholi. Thinner and/or laterally restricted LV-LD layers, as well as shorter LV-LD columns result in less uplift. Tholus width is similar to the LV-LD column width.

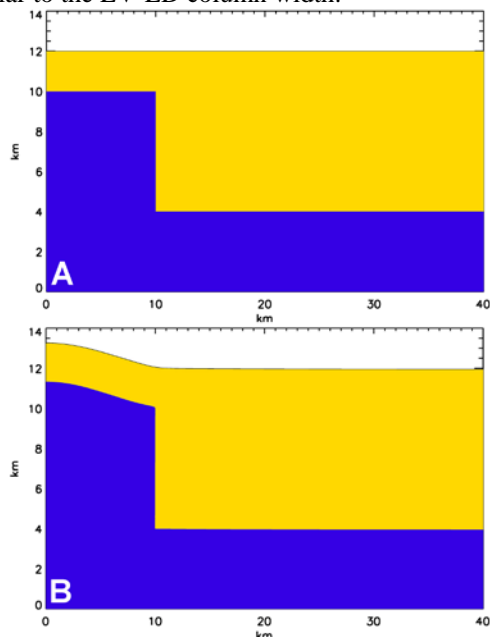


Figure 2: Axisymmetric finite element simulation of deformation resulting from a HV-HD crust (yellow) overlying a LV-LD layer (blue) of varying thickness. (A) Initial. (B). A 2-km high tholus results.

We also examine how surface topography from impact craters can drive flow of a LV-LD layer at depth (case 2). Figure 3 shows that a LV-LD layer beneath a portion of the crater can create a large tholus (3 km high) within the crater. The deformation is similar to Cosecha Tholus and the tholus in Begbabel crater (Fig. 1). The location and topographic amplitude of the resulting tholus again depends on the depth and lateral extent of the LV-LD layer.

Conclusions: Our preliminary investigation shows that solid-state deformation may be capable of creating Ceres' numerous tholi if the crust is heterogeneous at large scales. Buoyancy can bring low-density material to within 10-20 km of the surface, where differential loading drives flow capable of producing tholus-like surface features. This suggests prodigious cryovolcanism might be unnecessary for producing Ceres' tholi.

Acknowledgements: This work is supported by NASA's Dawn Guest Investigator Program.

References: [1] Ruesch O. et al. (2016) *Science*, 353, aaf4286. [2] Sori, M. M. et al. (2017) *GRL* 44. [3] Buczkowski et al. (2016) *Science* 353, aaf4332. [4] Sizemore, H. G. et al. (2018) *LSPC*. [5] Marchi S. et al. (2016) *Nat. Comm.* 7, 12257. [6] Adam J. B. et al. (2009) *Geology* 37, 691-694. [7] Hudek, M. R. and Jackson, M. P. A. (2007) *Earth Sci. Rev.* 82, 1-28. [8] Ermakov A. I. et al. (2017) *JGR* 122. [9] Bland M. T. et al. (2016) *Nat. Geo.* 9, 538-542. [10] Fu, R. R. et al. (2017) *EPSL* 476, 153-164. [11] Ammannito E. et al. (2016) *Science* 353, aaf4279. [12] Williams, D. A. (2018) *Icarus* in press. [13] Melosh, H. J. and Raefsky, A. (1980) *Geophys. J. R. astr. Soc.* 60, 333-354. [14] Schultz-Ela, D. D. et al. (1993) *Tectonophys.* 228, 275-312.

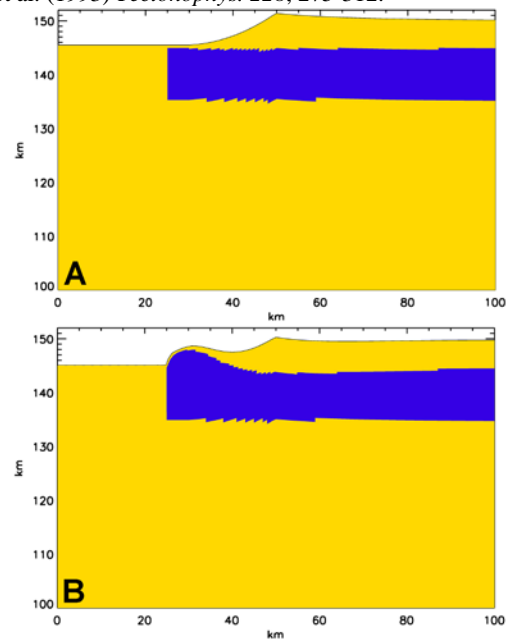


Figure 3: As in Fig. 2 but for a LV-LD layer partially underlying crater topography.